Bacterial defiance as a form of prodrug failure

Authors: Brandon Alexander Holt[1] and Gabriel A. Kwong[1—5,*]

Affiliations:

[1] Wallace H. Coulter Department of Biomedical Engineering, Georgia Tech College of - Engineering and Emory School of Medicine, Atlanta, GA 30332, USA; [2] Parker H. Petit Institute of Bioengineering and Bioscience, Atlanta, GA 30332, USA; [3] Institute for Electronics and Nanotechnology, Georgia Tech, Atlanta, GA 30332; [4] Integrated Cancer Research Center, Georgia Tech, Atlanta, GA, 30332; [5] Georgia ImmunoEngineering Consortium, Georgia Tech and Emory University, Atlanta, GA 30332.

[*]To whom correspondence should be addressed.

Address: 345 Ferst Dr, Atlanta, GA 30332

Phone: 404-385-3746

Email: gkwong@gatech.edu.

ABSTRACT

Classifying the mechanisms of antibiotic failure has led to the development of new treatment strategies for killing bacteria. Among the currently described mechanisms, which include resistance, persistence and tolerance, we propose *bacterial defiance* as a form of antibiotic failure specific to prodrugs. As a prototypic model of a bacteria-activated prodrug, we construct cationic antimicrobial peptides (AMP), which are charge neutralized until activated by a bacterial protease. This construct successfully eliminated the vast majority of bacteria populations, while localizing activity to bacterial membranes and maintaining low active drug concentration. However, we observed defiant bacteria populations, which survive in the presence of identical drug concentration and exposure time. Using a multi-rate kinetic feedback model, we show that bacteria switch between susceptibility and defiance under clinically relevant environmental (e.g., hyperthermia) and genetic (e.g., downregulated protease expression) conditions. From this model, we derive a dimensionless quantity (Bacterial Advantage Heuristic, *BAH*) – representing the balance between bacterial proliferation and prodrug activation – that perfectly classifies bacteria as defiant or susceptible across a broad range of conditions. To apply this concept to other classes of prodrugs, we expand this model to include both linear and nonlinear terms and use general pharmacokinetic parameters (e.g., half-life, EC50, etc.). Taken together, this model reveals an analogous dimensionless quantity (General Advantage Key, *GAK*), which can applied to prodrugs with different activation mechanisms. We envision that these studies will enable the development of more effective prodrugs to combat antibiotic resistance.

INTRODUCTION

The rise of multidrug-resistant infections coupled with the lack of newly developed antibiotics has created a serious public health threat [1,2]. Understanding the causes of antibiotic failure improves the development of new drugs and informs clinical treatment strategies [3-5]. These failure mechanisms are broadly classified into three distinct categories (e.g., resistance, persistence, and tolerance), which are characterized by the change in drug concentration and exposure time required to kill the bacteria [6]. For example, resistance is characterized by genetic mutations which result in bacteria requiring significantly higher concentrations of antibiotic (minimum inhibitory concentration, MIC) to be lethal. By contrast, bacteria exhibiting tolerance or persistence require increased drug exposure time (minimum duration for killing, MDK), with the latter exhibiting a biphasic killing profile. Further, bacteria populations become tolerant through environmental conditions or genetic mutations, whereas persistence is an actively-maintained, non-heritable state exhibited by a subpopulation of bacteria. Discriminating between these survival strategies employed by bacteria is crucial for the development of new drugs and clinical treatment decisions [6].

Antibiotic success is improved by proper drug titration, as overdosing leads to off-target toxicity and underdosing increases the likelihood of pathogens developing resistance[7,8]. However, ideal drug doses are difficult to achieve over the course of treatment because infection burden changes dynamically over time, creating a moving target[7-9]. Prodrugs, which represent 10% of all FDA-approved drugs in the last decade, are a promising solution because they are automatically titrated by a disease-related activation mechanism and reduce the risk of off-target effects [10]. Prodrugs, such as ganciclovir [11] and sultamicillin [12], are administered as a biologically inactive form and are enzymatically or chemically activated by the diseased cells or pathogens. Here, we create self-titrating prodrugs using cationic antimicrobial peptides (AMP), which evolved as a part of innate immunity and display broad-spectrum and prokaryote-specific antimicrobial properties

[13]. Cationic AMPs act by disrupting bacterial membranes and inducing inflammatory responses [14], but suffer from off-target effects (i.e., toxicity) and low stability *in vivo* [15,16]. Our AMP prodrugs are activated directly by proteases, a multifunctional class of enzymes that are responsible for regulating important health processes, such as immunity and blood homeostasis, and are major drivers of disease, including cancer and sepsis [17-21]. We chose to target bacterial proteases directly, which are a major cause of virulence [22,23] during infections and important targets for developing antibiotics [24]. Of these proteases, outer membrane protease T (OmpT), is a membrane-bound bacterial protein that is widely conserved across gram-negative bacteria of the *Enterobacteriaceae* family and recognizes a variety of targets that contribute to virulence (e.g., plasminogen)[25-27]. In this work, we design cationic AMPs that are locked by charge complexation with anionic peptides and connected with a protease-cleavable linker substrate [28,29]. We create a peptide linker recognized by *E. coli* protease OmpT, such that increasing concentrations of bacteria yield higher concentrations of free drug (**Fig. 1A**).

While this formulation eliminates the majority of bacteria, we observe bacteria populations that we named defiant, which proliferate in the presence of active drug by consistently outpacing prodrug activation at all stages of growth (i.e., log phase, stationary phase). To understand the mechanism by which bacteria become resistant to prodrugs, we built a system of coupled ODEs that model the dynamics of the bacteria-prodrug competition. We use this model to derive two dimensionless quantities – the Bacterial Advantage Heuristic (*B.A.H.*) and the General Advantage Key (*G.A.K.*) – which predict whether bacteria will become defiant under a broad range of conditions. At low *BAH* or *GAK* values, bacteria are susceptible to elimination, but after a critical threshold the bacteria switch to a state of defiance, in which the bacteria proliferate in the presence of activated drug (**Fig. 1B**). These quantitative mechanistic insights will better inform future drug design and treatment protocols leading to antibiotic success.

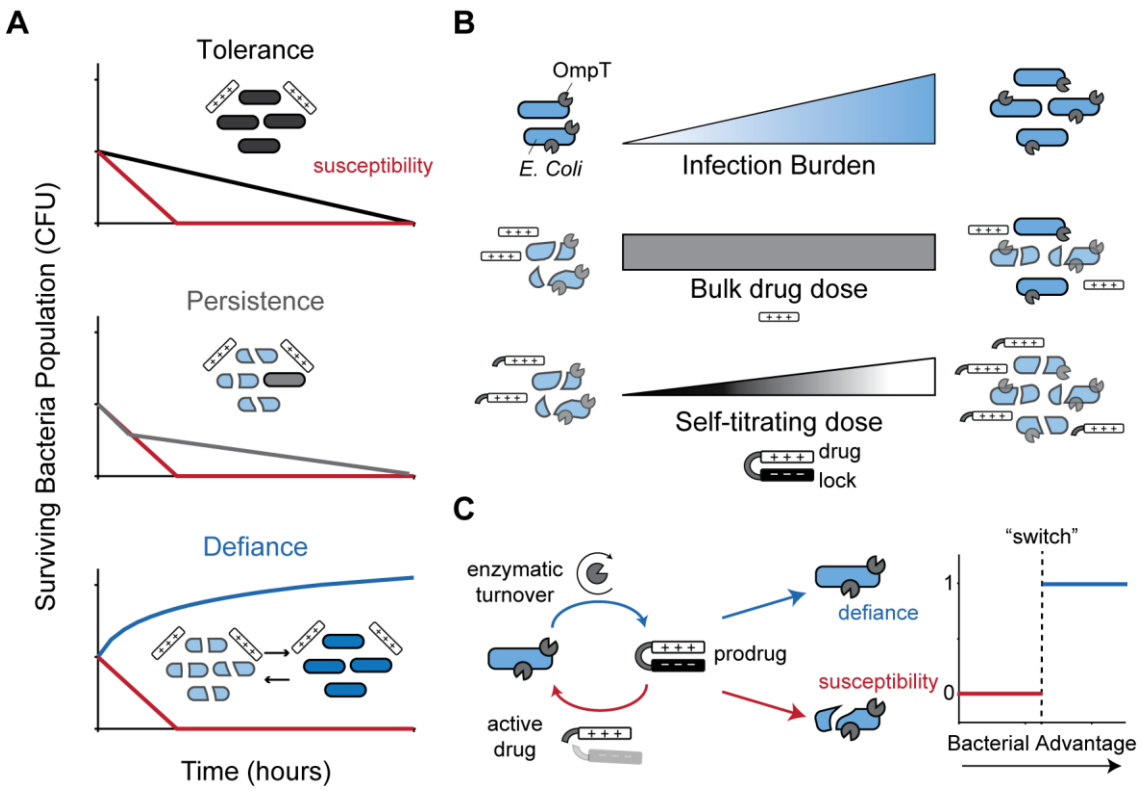

Fig. 1. Bacterial defiance in the context of self-titrating prodrugs (**A**) Schematic comparing time-dependent killing profiles of bacteria exhibiting tolerance, persistence, or defiance. (**B**) As infection burden increases (top), a static dose will result in an improper dose (middle). Conversely, a self-titrating drug will unlock an appropriate dose at all infection burdens (bottom). (**C**) Proliferating bacteria either be defiant or susceptible to the prodrug, where the two outcomes are strictly separated by a critical Bacterial Advantage Heuristic (*BAH*) value, resulting in switch-like behavior.

RESULTS & DISCUSSION

A bacteria-activatable prodrug targets *E. coli* protease OmpT

To create a bacteria-activated prodrug, we developed an antimicrobial peptide (AMP) that is activated by protease activity. This formulation consisted of a cationic AMP (polyarginine) in charge complexation with anionic peptide locks (polyglutamic acid) to create an inactive form of

the AMP[28]. The drug (polyarginine) and lock (polyglutamic acid) were connected with a linker peptide (RRSRRV) that is unlocked by a bacterial protease (OmpT) upon proteolytic cleavage, creating a precise mechanism for self-titration (**Fig. 2A**). To demonstrate the specificity of OmpT for the chosen linker peptide sequence, we synthesized a fluorescent quenched peptide[26] and detected OmpT activity via increasing fluorescent signal both with recombinant OmpT and with live *E. coli* culture. Further, we demonstrated the ability to turn off OmpT activity with the serine protease inhibitor, Aprotinin, which exhibits inhibitory effects in the micromolar range[25] (**Fig. 2B, C**). Using this substrate, we confirmed that the proteolytic cleavage of this substrate linker also occurred when docked on the drug-lock complex, which likely presents a different conformational state of the peptide substrate (**Fig. S1**). To determine the MIC of the unlocked drug, we showed that bacteria dosed with free drug show no growth in comparison to bacteria alone (**Fig 2D, E**). Dosing locked prodrug at this concentration, we used an orthogonal protease (Tobacco Etch Virus Protease) substrate pair to show the drug is only activated to kill bacteria in the presence of the correct target protease. We then used the prodrug locked with the OmpT substrate to show that the drug is only activated in the presence of bacterial protease activity. In the presence of the locked prodrug, all bacteria were eliminated whereas in the presence of the OmpT inhibitor, Aprotinin, bacteria proliferated at the same rate as the bacteria alone control (**Fig 2D, E, Table S1**).

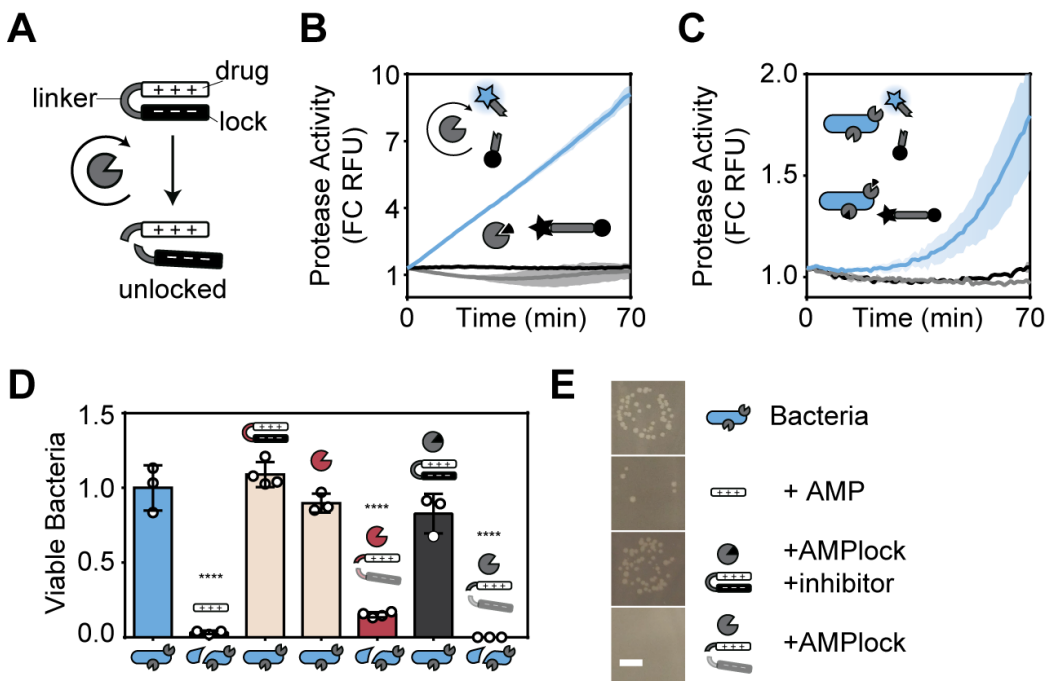

Fig. 2. A bacteria-activatable prodrug targets *E. coli* protease OmpT (**A**) A cationic AMP (drug) locked by an anionic peptide (lock) with a protease-cleavable linker is activated by enzyme activity. Cleavage assay measuring recombinant OmpT (grey protease) activity (**B**) and OmpT expressed by live E. coli (**C**) against a fluorescent quenched peptide substrate (blue lines). Negative control is with the addition of inhibitor aprotinin (black triangle, black lines). Probe only control (grey lines). Shading represents standard deviation (n = 3). (**D**) Bacteria viability assay quantifying the cytotoxic effect of the AMP-locked drug in the presence of the cognate active protease (TEV protease is red; OmpT is grey). Error bars represent standard deviation (n = 3). (**E**) Figure legend and representative images of bacterial plates used for estimating viability. (scale bar = 4 mm) * < 0.05, ** < 0.01, *** < 0.001, and **** < 0.0001.

Creating a bacteria prodrug ODE model

The bacteria-activated prodrug leveraged protease activity to enable precise titration according to a fixed rate constant (i.e., activated drug concentration per time), which is a function of system parameters, including enzymatic efficiency (k_{cat}/K_m) and bacterial growth rate (r). To quantitatively

understand how the rate of prodrug activation balances the number of living bacteria and the concentration of activated drug, we built a mathematical model using a system of nonlinear ordinary differential equations (ODE). We designed the high-level structure of our multi-rate model to include a negative feedback loop, where bacteria growth promotes prodrug activation, which in turn inhibits bacteria growth (**Fig. 3A**). We modeled the growth of the bacteria population, *B*, with a standard logistic growth model [30], where B_{max} determines the bacterial carrying capacity (maximum concentration of bacteria) and the growth rate, *r*, determines the speed at which the population approaches B_{max}. The decay of the bacteria population is a function of the concentration of unlocked drug, *U*, and the amount of drug needed to kill bacteria per unit time, *a* (**Table S2, Equation 1.1**).

$$\frac{dB}{dt} = rB\left(1 - \frac{B}{B_{\max}}\right) - \frac{U}{a} \tag{1.1}$$

The drug is unlocked by enzymatic activity, so we modeled the decay of the available locked drug, *L,* with standard Michaelis-Menten kinetics where the catalytic rate of the reaction and the half-maximal substrate concentration are determined by k_{cat} and K_m, respectively (**Equation 1.2**). We defined one bacterium, with ~ 2.5×10^3 OmpT proteases per cell [31], as equivalent to one effective enzyme to reflect the valency of protease active sites on each bacterial membrane.

$$\frac{dL}{dt} = -k_{cat} B \frac{L}{K_m + L} \tag{1.2}$$

The conversion from locked to unlocked drug, *U,* is conserved, so the decay of locked drug directly translates to the growth of unlocked drug. The decay of unlocked drug, a^*, is due to aggregation with dead bacteria membranes, for which we used published values [32] (**Equation 1.3**).

$$\frac{dU}{dt} = k_{cat} B \frac{L}{K_m + L} - \frac{a^*}{a} U \tag{1.3}$$

To fit this model to our data, we measured the parameters included in the model, including drug cytotoxicity (e.g., *EC50, a*), enzymatic efficiency (e.g., k_{cat}, K_m), and bacterial growth rate (*r*). To measure drug cytotoxicity, we quantified the percent of viable bacteria when exposed to unlocked AMP drug doses ranging from nanomolar to millimolar concentrations and observed a spike in cytotoxicity in the micromolar range (**Fig 3B**). To quantify enzymatic velocity, we measured proteolytic velocity (moles L^{-1} s^{-1}) under substrate concentrations ranging from 0—200 uM and fit the Michaelis-Menten equations to this data to calculate k_{cat} and K_m (**Fig 3C**). To calculate bacterial growth rate constants, we incubated bacteria in broth or water at 37C and measured OD_{600} over the course of 8 hours, revealing a higher growth rate in broth consistent with published values[30,33] (3.0 > 0.1 h^{-1}) (**Fig 3D**). Using these measured parameters (**Table S2**), we generated kinetic curves for bacteria number and drug concentration over time. The model showed that after a period of initial bacterial growth, the lagging drug population eliminated the infection burden. While the initial reservoir of locked drug concentration was ~200 µM, the unlocked drug never rose above 5 µM (**Fig. 3E**), revealing that this system maintains the minimal drug concentration required to kill the infection.

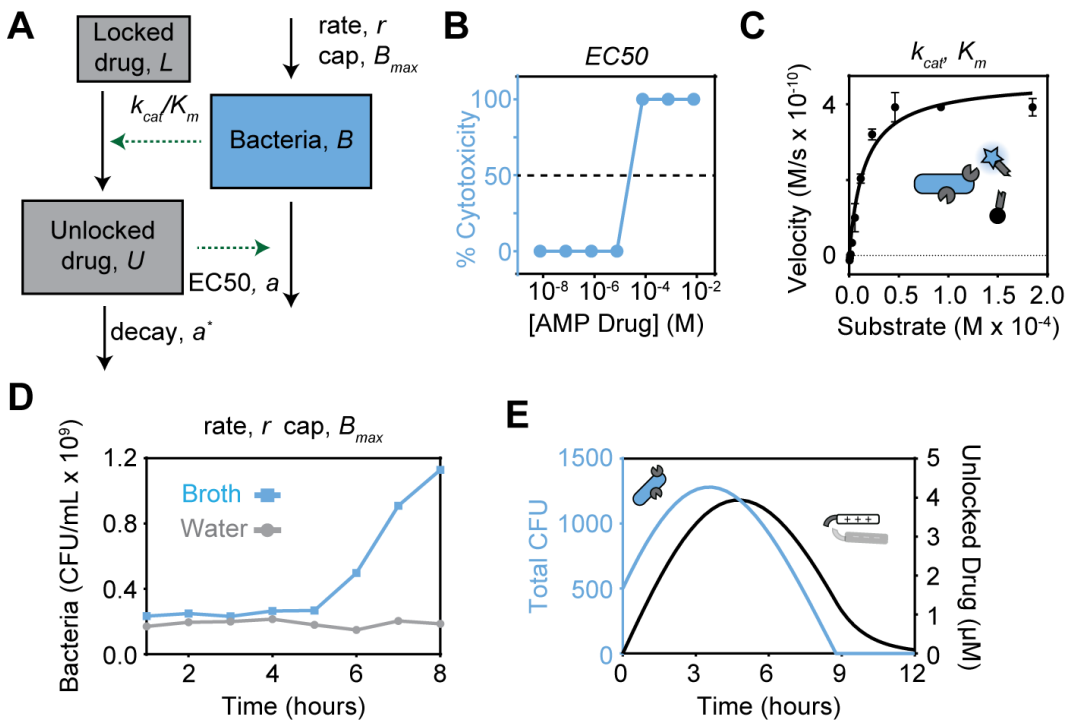

Fig. 3. Creating a bacteria prodrug ODE model. (**A**) Graphical representation of the model of bacteria and unlocked drug populations. (**B**) EC50 measurement on a sample of *E. coli* exposed to increasing concentrations of AMP. (**C**) Measuring k_{cat}/K_m from a series of cleavage assays incubating *E. coli* at a range of substrate concentrations. (**D**) Growth rate calculation of *E. Coli* in broth and water by measuring OD at 600 nm. (**E**) Predicting the dynamics of the bacteria and unlocked drug population given empirical parameter values. Error bars are standard deviation (n = 3).

Predicting bacterial defiance with a dimensionless constant

While it is advantageous for prodrugs to minimize the concentration of active drug, we show that this enables defiant populations of bacteria to appear under certain circumstances. We hypothesized that a critical relationship between the system parameters (e.g., k_{cat}/K_m, r, etc.) determines whether bacteria become defiant. From the governing equations, we derived a dimensionless quantity representing the balance between growth rate (r) and enzymatic turnover (k_{cat}/K_m), which we define as the Bacterial Advantage Heuristic (*B.A.H.*) (**Equation 1.4**).

$$B.A.H. = \log_{10}\left(\frac{r / B_{\max}}{k_{cat} / K_M}\right) \tag{1.4}$$

Under this definition, bacteria became defiant when they reach a critical *BAH* value, either through genetic or environmental changes. For example, as the bacteria grew faster (*r*), *BAH* increased because the bacteria were more likely to multiply before being killed by an activated drug. Conversely, the *BAH* decreased as bacterial enzyme activity (k_{cat}/K_m) increased, because the bacteria were more likely to be killed by an activated drug before multiplying. To find the critical *BAH* threshold that determined defiance, we set up nine different environmental conditions, each with a unique combination of k_{cat}/K_m and *r* values, which we controlled with ambient temperature, broth concentration and protease inhibitors. We incubated bacteria with the previously developed fluorophore-quencher probe (*P*, **Fig 2**) to monitor bacterial protease activity over time in each of the nine conditions. To quantify *r*, k_{cat}/K_m and *BAH*, we fit a simplified model of logistic bacteria growth and enzymatic turnover since there is no prodrug in this system (**Fig. 4A, Table S2**, **Equation 1.5, 1.6**).

$$\frac{dB}{dt} = rB\left(1 - \frac{B}{B_{\max}}\right) \tag{1.5}$$

$$\frac{dP}{dt} = -k_{cat} B \frac{P}{K_m + P} \tag{1.6}$$

To measure the outcome of bacteria populations exposed to the prodrug, we set up the same nine environmental conditions with the addition of the AMP prodrug (**Fig 3, Equations 1.1—1.3**). We found experimentally that the final bacteria population (i.e., steady-state value) was binary: either 0 or B_{max}, which is confirmed analytically because the steady state value of U_{ss} is always 0 (**Fig 4B**, **Equation 1.7, 1.8**).

$$0 = B' = rB_{ss}\left(1 - \frac{B_{ss}}{B_{\max}}\right) \tag{1.7}$$

$$B_{ss} = 0, B_{\max} \tag{1.8}$$

Therefore, our model predicted that a population of bacteria in the presence of a prodrug will converge to either susceptibility (death) or defiance (survival) (**Fig 4C**). To validate our model, we made serial CFU measurements and compared the data to our simulations, which correctly predicted the onset of defiance in each of the nine conditions (**Fig. 4D, Fig S2, Table S3**). We experimentally determined the critical *BAH* threshold by plotting the defiance versus the corresponding *BAH* value, which revealed a sharp step function (BAH_{crit} = 3.26). To confirm this result computationally, we simulated 10^4 unique *BAH*s by varying *r* and k_{cat}/K_m across four orders of magnitude and comparing to the simulated outcome (**Fig. 4E**). When using the *BAH* as a binary classifier of this system, we perfectly predicted the onset of bacterial defiance under a set of 13 unique environmental conditions (**Fig 4F, G**). Further, we switched defiant bacteria to a state of susceptibility by changing the amino acid sequence of the peptide linker to increase k_{cat}/K_m (**Fig S3**). This demonstrated the ability to improve prodrug success using design principles guided by a dimensionless quantity, *BAH*.

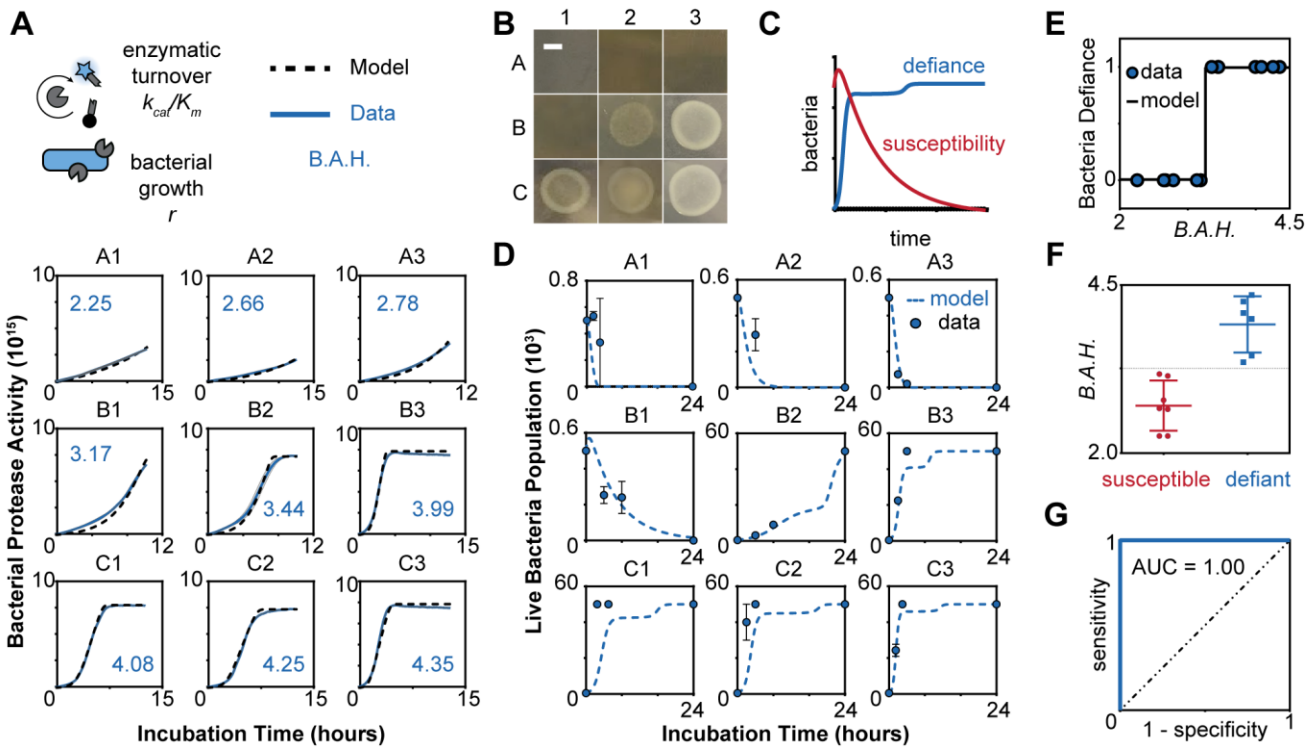

Fig. 4. Predicting bacterial defiance with a dimensionless constant (**A**) Bacterial cleavage assays, from which growth rate (r) and enzyme kinetics (k_{cat}/K_m) are extracted, and *BAH* is calculated (inset). (**B**) Agar plates showing presence/absence of bacterial growth and end-point for nine environmental conditions (A1—C3, scale bar = 4 mm). (**C**) Schematic depicting that bacterial defiance is characterized by proliferation in the presence of activated drug. (**D**) Validating the model with s erial CFU measurements (error bars SEM) and ODE model simulations of nine conditions given extracted growth rate and enzyme kinetics parameter values. (**E**) Correlating BAH with bacteria outcome to measure critical defiance value. (**F**) Grouping bacteria populations into defiant and susceptible based on *BAH*. (**G**) Using *BAH* to classify populations as defiant based on bacteria-driven parameters (*r* and k_{cat}/K_m).

A generalized model of disease-triggered prodrugs.

To apply the concept of bacterial defiance to a broad range of prodrugs, we developed a general form of the prodrug-disease target model. This model did not depend on the mechanism of action

(**Fig. 5A**) and raised each variable to an arbitrary power to allow for both linear and non-linear processes. In this system, we described a disease (*D*) which converts a prodrug (*P*) into an active form (*A*) by an arbitrary mechanism (**Equations 1.9—1.11**):

$$\frac{dD}{dt} = a\left(1 - \left(\frac{D}{D_{\max}}\right)^n\right) - bA \tag{1.9}$$

$$\frac{dP}{dt} = -cD^n P^n \tag{1.10}$$

$$\frac{dA}{dt} = cD^n P^n - dD^n A^n \tag{1.11}$$

We defined four generalized parameters: disease expansion rate (*a*), drug efficiency (*b*), drug activation rate (*c*), and drug decay (i.e., metabolism and excretion, *d*), which are well-established pharmacokinetic parameters for prodrugs. We defined a boundary condition based on the constraint that total drug concentration (i.e., prodrug + active drug) is always decreasing and is therefore less than the initial prodrug concentration, which must hold true for any time, *t* (**Equation 1.12**).

$$\begin{gathered} A(t) + P(t) \le P(t=0) \\ A_{ss} + P_{ss} \le P_0 \end{gathered} \tag{1.12}$$

By substituting the steady state values of *A* and *P* when *D* converges to 0, we defined an inequality that holds true when the disease is susceptible to the prodrug (i.e., $D_{ss} = 0$) (**Equation 1.13**).

$$\left(\frac{a}{b}\right)^{1/n} + \left(\frac{ad}{bc}\right)^{1/n} \le P_0 \tag{1.13}$$

Therefore, when the collective values of *a, b, c,* and *d* contradict this inequality, the disease will reach carrying capacity (D_{max}), which is a state of defiance. Using this condition, we defined a

dimensionless group, the General Advantage Key (*GAK*), which predicts the critical point at which diseases switch to a state of defiance (**Equation 14**).

$$G.A.K. = \ln\left[\frac{1}{P_0}\left(\frac{a}{b}\right)^{1/n} + \left(\frac{ad}{bc}\right)^{1/n}\right] > 0 \tag{1.14}$$

Therefore, high disease growth rates (*a*) and drug decay (*d*), coupled with low drug efficacy (*b*) and disease activity (*c*), result in defiance (*GAK* > 0). Our simulations showed that when the initial prodrug was considered non-limiting (i.e., $P_0 \gg {}^{ad}/_{bc}$), the disease switched states precisely at *GAK* = 0, but at limiting concentrations of P_0, susceptible diseases moving slowly towards elimination survived because the prodrug resource was depleted. As the starting amount of prodrug decreased, a larger fraction of systems with *GAK* < 0 entered the defiant state creating phase shifted step-functions. As we decreased P_0, the system entered the drug-limited regime faster for larger values of ${}^{ad}/_{bc}$, resulting in larger phase shifts (**Fig. 5B**). We extended the generalizability of this model to prodrug systems that operate under nonlinear processes and confirmed computationally that higher order models produce the same switch-like behavior centered around *GAK* = 0 (**Fig. 5C**). These parameters are fundamental pharmacokinetic quantities, which are measured for any FDA-approved prodrug. We envision the *GAK* to be used a guiding principle for designing prodrugs that combat antibiotic failure.

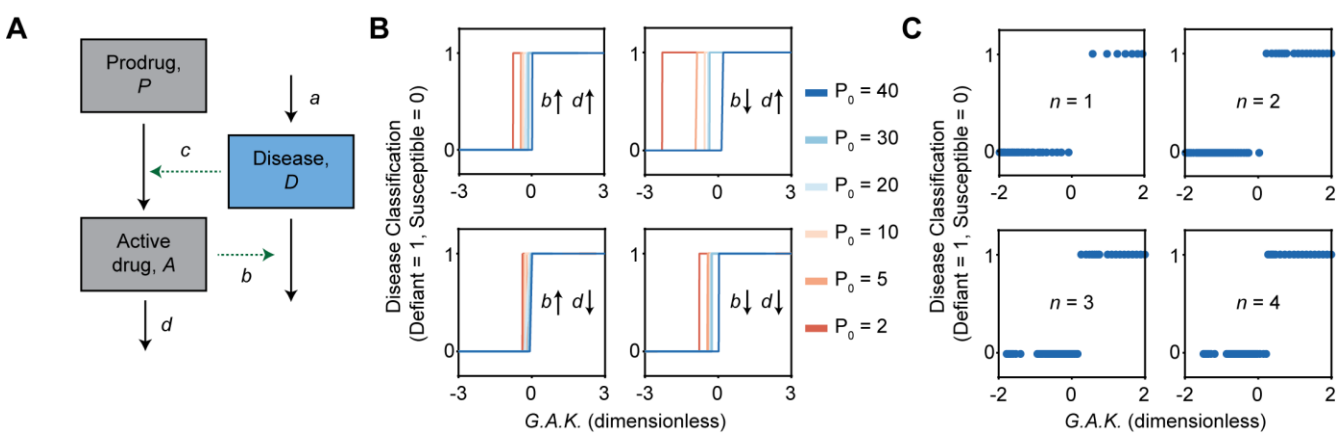

Fig. 5. A generalized model of disease-triggered prodrugs. (**A**) Schematic of generalized model of disease activated prodrug, with parameters *a* (disease growth), *b* (drug EC50), *c* (drug kinetics), and *d* (drug decay). (**B**) Computationally predicted disease outcomes from general form model, using *GAK* as a predictor for disease outcome. Each panel indicates the relative value of $^{ad}/_{bc}$ by increasing or decreasing *b* and *d* three-fold. Line color shifts from blue to red indicate decreasing amount of starting prodrug (P_0). (**C**) Simulating higher order nonlinear models to identify the value of *BAH* at which the system switches states.

CONCLUSION

Here, we studied bacterial defiance, a form of antibiotic failure which allows bacteria to proliferate while activating prodrugs. We created an OmpT-activatable AMP prodrug with the ability to localize its activity to *E. coli* membranes and elicit precise titration. This formulation can be applied to other diseases by designing a peptide linker specific to a disease-related protease. Due to the promiscuous nature of proteases, this platform may allow for rapid multiplexing, wherein multiple substrates are indexed to a library of candidate AMPs. In this context, we envision our template to be used for complex infections, wherein a library of possible AMPs may be administered and only those exposed to the proper protease signature will be unlocked. This template enables rapid engineering of diverse AMP prodrug libraries capable of targeting proteases, which are dominant drivers of disease [21].

We established a mathematical framework for determining the mechanism of defiance for bacteria and general diseases. Under this framework, measurable system parameters determine whether bacteria will become defiant in the presence of a particular prodrug. Here, we controlled the development of defiance with environmental conditions affecting bacterial growth rate and enzymatic turnover. Previous studies examining enzyme-activated prodrugs corroborate this issue and therapeutic solutions use substrate-focused engineering strategies, which is limited by

the ability to discover better substrates[34,35]. Our model reveals that there are many parameters, including drug half-life and temperature, that can be controlled to improve prodrug efficacy. In addition to these environmental conditions, there are established genetic mutations in *E. coli* capable of causing defiance. For example, mutations resulting in partial reduction or total loss of OmpT activity [36,37] as well as changes in growth rate [33] have been identified in *E. coli*. This model predicts the onset of bacterial defiance in a well-defined system, enabling more informed experimentation and potential therapeutic strategies.

These findings complement existing knowledge about bacterial mechanisms that cause antibiotic failure. Physiologically, bacterial defiance is most likely to surface as a populational state, either through environmental or genetic changes, which most closely resembles tolerance. Conversely, individual bacteria may become defiant, either through irregular phenotypic regulation of growth rates or particular enzymes, similar to phenotypic resistance. By contrast, tolerance is generally associated with bacteria slowing down essential processes, such as growth or metabolism, in direct contrast to the demonstrated mechanism by which bacteria become defiant [6]. Phenotypic resistance describes specific situations, such as growth in biofilms or a stationary growth phase [38]. The current definitions and clinical practices used to identify and treat these mechanisms do not fit precisely with the characteristics of bacterial defiance [6], motivating the classification of these phenomena in the presence of prodrugs. The proposed framework for characterizing defiance will enable more conscious engineering of prodrugs and provide strategies for combatting antibiotic failure.

Author Contributions: G.A.K. and B.A.H conceived of the idea, designed experiments and interpreted results, and wrote the manuscript. B.A.H. carried out experiments.

Acknowledgments: This work was funded by an NIH Director's New Innovator Award (Award No. DP2HD091793). B.A.H is supported by the NSF GRFP, National Institutes of Health GT BioMAT Training Grant under Award Number 5T32EB006343 and the Georgia Tech President's Fellowship. This material is based upon work supported by the National Science Foundation Graduate Research Fellowship under Grant No. DGE-1650044 (B.A.H.). G.A.K. holds a Career

Award at the Scientific Interface from the Burroughs Welcome Fund. The content is solely the responsibility of the authors and does not necessarily represent the official views of the National Institutes of Health. The authors would like to thank Ian Miller (Georgia Tech), Shreyas Dahotre (Georgia Tech), and Dr. Kyle Allison (Georgia Tech & Emory) for their helpful discussion.

EXPERIMENTAL PROCEDURES

Protease Cleavage Assays

All protease cleavage assays were performed with a BioTek Cytation 5 Imaging Plate Reader, taking fluorescent measurements at 485/528 nm (excitation/emission) for read-outs measuring peptide substrates terminated with FITC (Fluorescein isothiocyanate). Kinetic measurements were taken every minute over the course of 60 – 120 minutes at 37 C. Tobacco Etch Virus protease (TEVp), along with its substrate and buffer was obtained from Anaspec, Inc. (Fremont, CA). Activity RFU measurements were normalized to time 0 measurement, and as such represent fold change in signal. Outer Membrane Protease T (i.e., OmpT, Protease 7) was purchased from Lifespan Biosciences (Seattle, WA). OmpT fluorescent peptide substrate was custom ordered from Genscript (Piscataway, NJ).

Bacterial culture and cytotoxicity measurement

DH5α Escherichia coli were a gift from Todd Sulchek's BioMEMS lab at Georgia Tech. E. coli were cultured in LB broth (Lennox) at 37 C and plated on LB agar (Lennox) plates. LB broth was purchasd from Millipore Sigma (Burlington, MA) and LB agar was purchased from Invitrogen (Carlsbad, CA). AMP and locked AMP were custom ordered from Genscript (Piscataway, NJ). See Table S1 for more information. Bacteria were grown to a concentration of 10^9 CFU/mL before being used for experiments. Concentration was estimated by measuring the OD_{600} of the bacterial suspension, and assuming an OD_{600} of 1.000 corresponds to a concentration of 8×10^8 CFU/mL. Bacterial cell viability was measured by making eight 10-fold serial dilutions, and plating three 10 uL spots on an LB agar plate. Plates were incubated overnight at 37C, and CFUs were counted. Untreated bacteria CFU counts served as control for 0% cytotoxicity, and bacteria + IPA (or 0 countable CFUs) served as control for 100% cytotoxicity.

Computational model

The ODE modelling and solutions were performed in MATLAB 2016b. Code can be found in supplementary information.

Statistical Analysis

Statistical analysis was performed using statistical packages included in GraphPad Prism 6. To assess the significance of increase in signal due to protease cleavage, we used a two-way ANOVA (without repeated measures) followed by Sidak's multiple comparisons test. A one-way ANOVA followed by Dunnett's multiple comparisons test was used to compare experimental means to cells only control bacterial viability assays. Two-way ANOVA followed by Sidak's multiple comparisons test used to compare experimental means to control for bacterial cytotoxicity at multiple starting concentrations.

SUPPLEMENTARY FIGURES AND TABLES

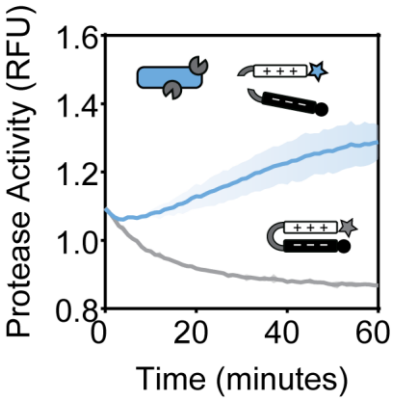

Fig. S1. Monitoring activation of AMP prodrug. Cleavage assay of bacteria cutting fluorescently labeled AMP prodrug.

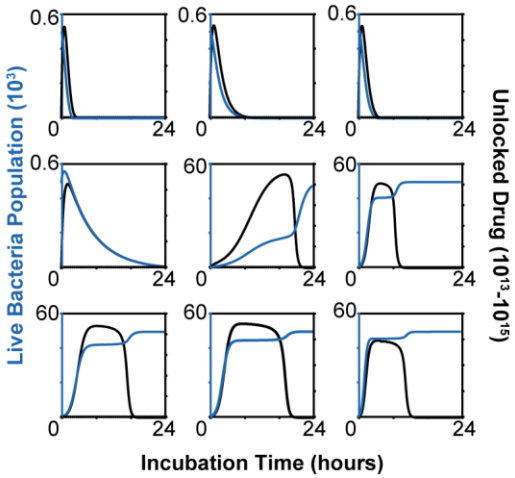

Fig. S2. Modeling bacteria and drug kinetics. ODE model of bacteria and unlocked drug populations over 24 hours for nine environmental conditions (Table S2).

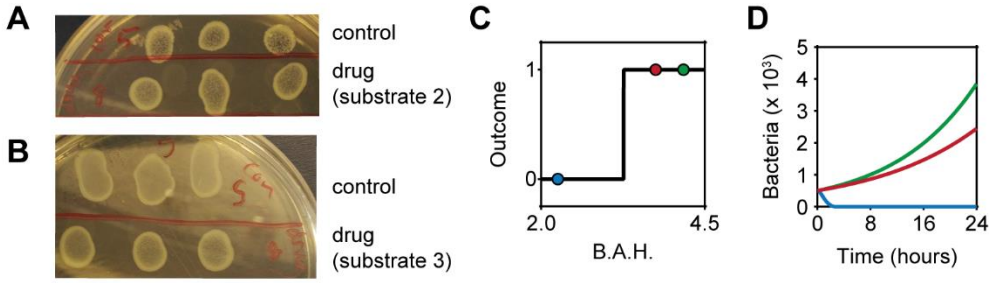

Fig. S3. Altering drug efficacy with substrate affinity. Bacteria viability plates post 24 hour incubation with drug unlocked by (A) substrate two and (B) substrate three. (C) B.A.H. values

extrapolated from bacteria + probe velocity measurements fitted to model. (D) Bacteria dynamics predicted by model given three different enzyme kinetics.

TABLE S1

Name	Peptide Sequence
Locked AMP (substrate 1)	EEEEEEEEEEEEERRSRRVRRRRRRRRR
Locked AMP (substrate 2)	EEEEEEEEEEERKTRRRRRRRRR
Locked AMP (substrate 3)	EEEEEEEEENLYFQGRRRRRRRRR
Locked AMP Probe	DABCYL-EEEEEEEEEEEEERRSRRVRRRRRRRRR[Lys(5-FAM)]
OmpT Probe	DABCYL-RRSRRV-Lys(5-FAM)

TABLE S2

Variable	Value	Units	Notes
r	0.1—3	h^{-1}	Bacterial growth rate
kcat	1—25e10	h^{-1}	Enzyme catalytic turnover
Km	4.5e14	[n] in 50 µL	Michaelis constant
Bmax	50,000	[n], bacteria	Bacteria carrying capacity
a	1e11	h^{-1}, AMP/bacteria/hr	Cytotoxic efficiency, EC50
a^*	2.4e11	AMP/bacteria	AMP decay

TABLE S3

Location (row, column)	Temperature	LB Broth Concentration	r (h^{-1})	k_{cat} (h^{-1}) x 10^{10}
1,1 (A1)	37C	0%	0.1	25
1,2 (A2)	30C	2%	0.14	13.6
1,3 (A3)	37C	2%	0.3	22
2,1 (B1)	37C	4%	0.5	15
2,2 (B2)	37C	6%	0.85	13.6
2,3 (B3)	37C	20%	2.2	1
3,1 (C1)	30C	20%	1.4	5.2
3,2 (C2)	30C	66%	1.6	4
3,3 (C3)	37C	66%	3	6

REFERENCES

1 Baquero, F., Martinez, J. L. & Canton, R. Antibiotics and antibiotic resistance in water environments. *Current opinion in biotechnology* **19**, 260-265, doi:10.1016/j.copbio.2008.05.006 (2008).

2 Gullberg, E. *et al.* Selection of Resistant Bacteria at Very Low Antibiotic Concentrations. *PLOS Pathogens* **7**, e1002158, doi:10.1371/journal.ppat.1002158 (2011).

3 Molina-Quiroz, R. C. *et al.* Cyclic AMP Regulates Bacterial Persistence through Repression of the Oxidative Stress Response and SOS-Dependent DNA Repair in Uropathogenic Escherichia coli. *mBio* **9**, doi:10.1128/mBio.02144-17 (2018).

4 Cohen, N. R., Lobritz, M. A. & Collins, J. J. Microbial persistence and the road to drug resistance. *Cell host & microbe* **13**, 632-642, doi:10.1016/j.chom.2013.05.009 (2013).

5 Allison, K. R., Brynildsen, M. P. & Collins, J. J. Metabolite-enabled eradication of bacterial persisters by aminoglycosides. *Nature* **473**, 216, doi:10.1038/nature10069

https://www.nature.com/articles/nature10069#supplementary-information (2011).

6 Brauner, A., Fridman, O., Gefen, O. & Balaban, N. Q. Distinguishing between resistance, tolerance and persistence to antibiotic treatment. *Nature Reviews Microbiology* **14**, 320, doi:10.1038/nrmicro.2016.34 (2016).

7 Bielicki, J. A. *et al.* Not too little, not too much: problems of selecting oral antibiotic dose for children. *BMJ : British Medical Journal* **351**, doi:10.1136/bmj.h5447 (2015).

8 Bailey, A. M., Stephan, M., Weant, K. A. & Justice, S. B. Dosing of Appropriate Antibiotics and Time to Administration of First Doses in the Pediatric Emergency Department. *The journal of pediatric pharmacology and therapeutics : JPPT : the official journal of PPAG* **20**, 309-315, doi:10.5863/1551-6776-20.4.309 (2015).

9 Iizumi, T., Battaglia, T., Ruiz, V. & Perez Perez, G. I. Gut Microbiome and Antibiotics. *Archives of medical research* **48**, 727-734, doi:10.1016/j.arcmed.2017.11.004 (2017).

10 Rautio, J., Meanwell, N. A., Di, L. & Hageman, M. J. The expanding role of prodrugs in contemporary drug design and development. *Nature Reviews Drug Discovery* **17**, 559, doi:10.1038/nrd.2018.46

https://www.nature.com/articles/nrd.2018.46#supplementary-information (2018).

11 Al-Badr, A. A. & Ajarim, T. D. S. in *Profiles of Drug Substances, Excipients and Related Methodology* Vol. 43 (ed Harry G. Brittain) 1-208 (Academic Press, 2018).

12 Baltzer, B. *et al.* Mutual pro-drugs of beta-lactam antibiotics and beta-lactamase inhibitors. *J Antibiot (Tokyo)* **33**, 1183-1192 (1980).

13 Zhang, L.-j. & Gallo, R. L. Antimicrobial peptides. *Current Biology* **26**, R14-R19, doi:https://doi.org/10.1016/j.cub.2015.11.017 (2016).

14 Mahlapuu, M., Håkansson, J., Ringstad, L. & Björn, C. Antimicrobial Peptides: An Emerging Category of Therapeutic Agents. *Frontiers in Cellular and Infection Microbiology* **6**, doi:10.3389/fcimb.2016.00194 (2016).

15 Wimley, W. C. & Hristova, K. Antimicrobial Peptides: Successes, Challenges and Unanswered Questions. **239**, 27-34, doi:10.1007/s00232-011-9343-0 (2011).

16 Bradshaw, J. Cationic antimicrobial peptides : issues for potential clinical use. *BioDrugs : clinical immunotherapeutics, biopharmaceuticals and gene therapy* **17**, 233-240 (2003).

17 Kwong, G. A. *et al.* Mass-encoded synthetic biomarkers for multiplexed urinary monitoring of disease. *Nat Biotech* **31**, 63-70, doi:http://www.nature.com/nbt/journal/v31/n1/abs/nbt.2464.html#supplementary-information (2013).

18 Holt, B. A. *et al.* Fc microparticles can modulate the physical extent and magnitude of complement activity. *Biomaterials science* **5**, 463-474, doi:10.1039/c6bm00608f (2017).
19 Holt, B. A., Mac, Q. D. & Kwong, G. A. Nanosensors to Detect Protease Activity In Vivo for Noninvasive Diagnostics. *JoVE*, e57937, doi:doi:10.3791/57937 (2018).
20 Mac, Q. D. *et al.* Non-invasive early detection of acute transplant rejection via nanosensors of granzyme B activity. *Nature biomedical engineering*, doi:10.1038/s41551-019-0358-7 (2019).
21 Lopez-Otin, C. & Bond, J. S. Proteases: multifunctional enzymes in life and disease. *The Journal of biological chemistry* **283**, 30433-30437, doi:10.1074/jbc.R800035200 (2008).
22 Frees, D., Brondsted, L. & Ingmer, H. Bacterial proteases and virulence. *Sub-cellular biochemistry* **66**, 161-192, doi:10.1007/978-94-007-5940-4_7 (2013).
23 Ingmer, H. & Brondsted, L. Proteases in bacterial pathogenesis. *Research in microbiology* **160**, 704-710, doi:10.1016/j.resmic.2009.08.017 (2009).
24 Culp, E. & Wright, G. D. Bacterial proteases, untapped antimicrobial drug targets. *The Journal Of Antibiotics* **70**, 366, doi:10.1038/ja.2016.138 (2016).
25 Brannon, J. R. *et al.* Inhibition of outer membrane proteases of the omptin family by aprotinin. *Infection and immunity* **83**, 2300-2311, doi:10.1128/IAI.00136-15 (2015).
26 McCarter, J. D. *et al.* Substrate Specificity of the Escherichia coli Outer Membrane Protease OmpT. *Journal of Bacteriology* **186**, 5919-5925, doi:10.1128/JB.186.17.5919-5925.2004 (2004).
27 Grodberg, J. & Dunn, J. J. ompT encodes the Escherichia coli outer membrane protease that cleaves T7 RNA polymerase during purification. *Journal of Bacteriology* **170**, 1245-1253 (1988).
28 Olson, E. S. *et al.* In vivo characterization of activatable cell penetrating peptides for targeting protease activity in cancer. *Integrative biology : quantitative biosciences from nano to macro* **1**, 382-393, doi:10.1039/b904890a (2009).
29 Franzman, M. R. *et al.* Targeted antimicrobial activity of a specific IgG-SMAP28 conjugate against Porphyromonas gingivalis in a mixed culture. *International journal of antimicrobial agents* **33**, 14-20, doi:10.1016/j.ijantimicag.2008.05.021 (2009).
30 Fujikawa, H., Kai, A. & Morozumi, S. A new logistic model for bacterial growth. *Shokuhin eiseigaku zasshi. Journal of the Food Hygienic Society of Japan* **44**, 155-160 (2003).
31 Ishihama, Y. *et al.* Protein abundance profiling of the Escherichia coli cytosol. *BMC Genomics* **9**, 102, doi:10.1186/1471-2164-9-102 (2008).
32 Roversi, D. *et al.* How Many Antimicrobial Peptide Molecules Kill a Bacterium? The Case of PMAP-23. *ACS Chemical Biology* **9**, 2003-2007, doi:10.1021/cb500426r (2014).
33 Jin, D. J., Cagliero, C. & Zhou, Y. N. Growth rate regulation in Escherichia coli. *FEMS microbiology reviews* **36**, 269-287, doi:10.1111/j.1574-6976.2011.00279.x (2012).
34 Barak, Y. *et al.* New enzyme for reductive cancer chemotherapy, YieF, and its improvement by directed evolution. *Molecular cancer therapeutics* **5**, 97-103, doi:10.1158/1535-7163.mct-05-0365 (2006).
35 Jordan, A. M., Khan, T. H., Osborn, H. M., Photiou, A. & Riley, P. A. Melanocyte-directed enzyme prodrug therapy (MDEPT): development of a targeted treatment for malignant melanoma. *Bioorganic & medicinal chemistry* **7**, 1775-1780 (1999).
36 Kramer, R. A., Zandwijken, D., Egmond, M. R. & Dekker, N. In vitro folding, purification and characterization of Escherichia coli outer membrane protease ompT. *European journal of biochemistry* **267**, 885-893 (2000).
37 Kramer, R. A. *et al.* Identification of essential acidic residues of outer membrane protease OmpT supports a novel active site. *FEBS letters* **505**, 426-430 (2001).
38 Corona, F. & Martinez, J. L. Phenotypic Resistance to Antibiotics. *Antibiotics (Basel, Switzerland)* **2**, 237-255, doi:10.3390/antibiotics2020237 (2013).